

# A deep *ROSAT* survey - XII. The X-ray spectra of faint *ROSAT* sources

O. Almaini<sup>1</sup>\*, T. Shanks<sup>1</sup>, B.J. Boyle<sup>2</sup>, R.E. Griffiths<sup>3</sup>, N. Roche<sup>3</sup>,  
G.C. Stewart<sup>4</sup>, and I. Georgantopoulos<sup>4</sup>

<sup>1</sup>Department of Physics, University of Durham, South Road, Durham, DH1 3LE, UK.

<sup>2</sup>Royal Greenwich Observatory, Madingley Road, Cambridge, CB3 0EZ, UK.

<sup>3</sup>Johns Hopkins University, Homewood Campus, Baltimore MA21260, USA.

<sup>4</sup>Department of Physics, University of Leicester, University of Leicester, LE1 7RH, UK.

Accepted May 16th 1996. Submitted November 14th 1995.

## ABSTRACT

Optical spectroscopy has enabled us to identify the optical counterparts to over 200 faint X-ray sources to a flux limit of  $S_{(0.5-2\text{keV})} = 4 \times 10^{-15} \text{ erg s}^{-1} \text{ cm}^{-2}$  on 5 deep *ROSAT* fields. Here we present a spectral analysis of all the X-ray sources to investigate claims that the average source spectra harden at faint X-ray flux. From a hardness ratio analysis we confirm that the average spectra from 0.5 – 2 keV harden from an equivalent photon index of  $\Gamma = 2.2$  at  $S_{(0.5-2\text{keV})} = 1 \times 10^{-13} \text{ erg s}^{-1} \text{ cm}^{-2}$  to  $\Gamma \simeq 1.7$  below  $1 \times 10^{-14} \text{ erg s}^{-1} \text{ cm}^{-2}$ . These spectral changes are due to the emergence of an unidentified source population rather than the class of X-ray QSOs already identified. The 128 QSOs detected so far show no evidence for spectral hardening over this energy range and retain a mean photon index of  $\Gamma = 2.2$ . Recent work suggests that many of the remaining unidentified sources are X-ray luminous galaxies. Taking a subset identified as the most likely galaxy candidates we find that these show significantly harder spectra than QSOs. The emission line galaxies in particular show spectra more consistent with the residual X-ray background, with  $\Gamma = 1.51 \pm 0.1$  from 0.1 – 2 keV. Individually the galaxies appear to be a mixture of absorbed and unabsorbed X-ray sources. Combined with recent cross-correlation results and work on the source number count distribution, these results suggest that we may be uncovering the missing hard component of the cosmic X-ray background.

**Key words:** galaxies: active – quasars: general - X-rays:general - X-rays: galaxies - diffuse radiation X-rays: general

## 1 INTRODUCTION

We are conducting a survey to understand the nature of the faint X-ray sources identified on deep (21 – 49 ks) *ROSAT* PSPC exposures. So far we have identified over 100 QSOs from 5 *ROSAT* fields and shown that QSOs make up at least  $\sim 30\%$  of the X-ray background (XRB) at 1 keV (Shanks et al 1991). However, studies of the QSO X-ray luminosity function (Boyle et al 1994) and the number count distribution (Georgantopoulos et al 1995) suggest that the known QSO population is unlikely to form more than 50% of the total XRB flux. QSOs also show relatively steep X-ray spectra with indices of  $\Gamma = 2.2 \pm 0.1$  while the extragalactic XRB

from 1-10 keV has a flatter power-law index of  $\Gamma = 1.4$  (Gendreau et al 1995). This suggests that we need a new, faint source population with a flatter X-ray spectrum to account for the remainder of the background radiation.

From these deep *ROSAT* exposures it is also beginning to emerge that many of the remaining X-ray sources are associated with faint galaxies. These appear to be a mixture of absorption and emission line galaxies with optical spectra and redshifts typical of the galaxy population, but the implied X-ray luminosities are 10 – 100 times higher than those of similar galaxies locally (Roche et al 1995a, Boyle et al 1995a, Griffiths et al 1995a, Carballo et al 1995, McHardy et al 1995). The nature of the X-ray emission mechanism in these galaxies is still not clear, but recent work at brighter flux limits (Boyle et al 1995b) suggests that some may be Seyfert 2 or starburst galaxies. The clearest evidence that

\* Present address: Institute Of Astronomy, Madingley Road, Cambridge CB3 OHA

faint galaxies are significant contributors to the XRB has come from the spatial cross-correlation of XRB fluctuations and faint  $B < 23$  galaxies (Roche et al 1995a). This statistical method avoids the source confusion problem that prevents faint galaxies from being associated with X-ray sources. The amplitude of the cross-correlation implies that  $B < 23$  galaxies directly contribute some  $17 \pm 2\%$  of the 1keV XRB. Integrating the implied local X-ray volume emissivity to faint magnitudes and high redshifts suggests that the remainder of the soft XRB can be explained by faint galaxies (Roche et al 1995a, Almaini 1996). Their potential contribution to the hard XRB depends critically on their X-ray spectra.

In this paper we investigate the X-ray spectra of all the sources identified on 5 deep *ROSAT* fields. Recent work by Carballo et al (1995) has suggested that X-ray luminous galaxies show harder spectra than QSOs. Other deeper surveys (Hasinger et al 1993, Vikhlinin et al 1994) have revealed the possibility that the mean spectra of the source population may harden as we go to fainter X-ray fluxes, perhaps indicating that we are beginning to identify the missing faint sources required to explain the remainder of the X-ray background. In this paper we attempt to identify the type of source responsible for this trend. In section 2 we present our data set and the data reduction techniques and in section 3 we use model independent hardness ratios to investigate the X-ray spectra of the QSOs and other source types. In section 4 we repeat this analysis with full spectral fitting followed by our conclusions and a discussion in section 5.

## 2 OBSERVATIONAL DATA

### 2.1 The sample

Here we use 5 deep (21 – 49 ks) pointed observations with the *ROSAT* PSPC with optical identifications from the X-ray source catalogue of Shanks et al 1996 (in preparation). These are well studied optical fields selected from the ultraviolet excess (UVX) survey of Boyle et al (1990). Our analysis is restricted to the central 18 arcminute radius of the *ROSAT* pointings to maximise the sensitivity of our observations since the point spread function of the PSPC rapidly increases beyond the central 20 arcminute radius. Due to the considerable contamination from both the galactic background and solar scattered X-rays below 0.5 keV (Snowden & Freyberg 1993) we optimize the sensitivity of source detection by concentrating on the 0.5-2.0 keV data.

Full details of the X-ray source detections and optical spectroscopic identifications will be given elsewhere (Shanks et al, in preparation) and so only brief details will be given below. Sources were identified using the standard PSS algorithm within the *ASTERIX* data processing package, which detects peaks above a certain threshold and matches the expected PSF to the background fluctuations to determine whether the source is real. In this way, 356 X-ray sources were detected above a  $4\sigma$  significance and 197 sources were detected above  $5\sigma$  in the 0.5-2.0 keV band over 5 *ROSAT* fields. Optical counterparts to these X-ray sources were identified from COSMOS and APM measurements of J and U band UK Schmidt plates. Astrometric transforms between *ROSAT* X-ray and COSMOS/APM co-ordinates were set

**Table 1.** Summary of optical identifications to  $4\sigma$  X-ray sources from 5 deep *ROSAT* fields.

AGN	128
Stars	27
Continuum	10
Clusters	1
Unobserved	96
Unidentified	89
(Probable galaxies)	(23)
Total	356

up using the Durham/AAT UVX QSOs detected by *ROSAT* on each field. Low resolution (12Å) optical spectra were then obtained for the nearest optical counterpart to each X-ray source using the AUTOFIB multi-object system at the Anglo-Australian Telescope. A summary of the optical identifications of the  $4\sigma$  sources is given in Table 1. Note that this is considerably less complete than the identifications of the smaller list of  $5\sigma$  sources listed in Georgantopoulos et al (1996) since in this work we are attempting to probe fainter flux limits. Of the 257 sources for which optical identifications were attempted, 128 were identified as QSOs and Seyfert 1 galaxies which directly account for  $\sim 30\%$  of the total XRB at 1keV (Shanks et al 1991). Less than 10% of the sources were found to be galactic late type stars. Of the remaining positive identifications, 10 continuum objects and the emission from a galaxy cluster were also detected (Roche et al 1995b). However, as can be seen from Table 1, a large fraction of the sources remain unidentified or unobserved (both hereafter referred to as the “unidentified” sources). In many cases, observing limitations prevented the object from being observed or the S/N in the optical spectra was too poor to allow a reliable identification. Interestingly however,  $\sim 100$  of these unidentified X-ray sources appeared to be associated with faint, “normal” galaxies on photographic plates and for 38 of these sources the optical counterpart was firmly identified as a galaxy by spectroscopy. However, due to the high sky density of galaxies at faint magnitudes ( $\sim 10000 \text{ deg}^{-2}$  at  $B < 23$ , Metcalfe et al 1991) and the  $\sim 25''$  FWHM X-ray error circle many of these will be chance coincidences. A reliable estimate of the contribution of faint galaxies to the XRB can only be determined statistically (see Roche et al 1995a). For the galaxies at brighter limiting magnitudes the confusion problem becomes less pronounced. We therefore identify a sample of “probable” galaxy candidates with  $B < 21.5$  for which the optical counterpart lies within  $20''$  of the X-ray source. This optical magnitude represents the limit of reliable galaxy identification on a UK Schmidt plate. Cross-correlating COSMOS and APM galaxy catalogues to the same magnitude limit with the unidentified X-ray sources we estimate that  $\sim 6$  of this restricted sample will be spurious identifications. 15 of these galaxies were identified with narrow emission line features and 8 were identified as absorption line galaxies. The sample used by Griffiths et al 1995b is taken from the  $5\sigma$  subset of these galaxies. Further details of the properties of these sources are given in Table 5 and in Shanks et al 1996.

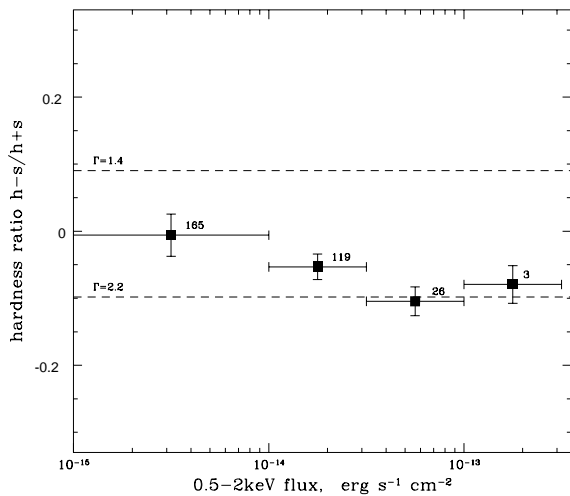


**Figure 1.** 0.5 – 2 keV hardness ratios for the stacked spectra of 313 X-ray sources from 5 deep *ROSAT* fields binned according to flux. The number of X-ray sources within each bin is indicated. For comparison, the hardness ratios for 2 power law models are also shown.

## 2.2 Obtaining X-ray spectra

For each source the X-ray counts used to determine fluxes, hardness ratios and spectra were obtained using a circle that encloses 90% of the source photons. The radius of this circle varies with energy and the off axis angle (Hasinger et al 1992). Data from periods of high particle background were excluded from the analysis, excluding approximately 10% of the data when the Master Veto Rate was above 170 counts  $s^{-1}$  (Plucinsky et al 1993). Due to the faint nature of many of these sources, considerable care was taken in choosing an area for background subtraction. Possible problems include irregularities in the galactic background or contamination from solar scattered X-rays. However, after the subtraction of sources the residual background levels were found to remain constant over the 18 arcminute central region and no significant gradient was apparent on any field. Circular areas of 4 to 6 arcminute radius were then chosen from source free regions to perform the background subtraction, correcting for the vignetting between source and background boxes.

## 3 HARDNESS RATIOS

### 3.1 QSOs and unidentified sources

Since the majority of our sources have fewer than 100 total counts in the *ROSAT* band, detailed spectral fitting is not possible. We therefore derive model independent hardness ratios to compare the spectral properties of these sources. By forming a “soft” energy band ( $S$ ) from the 0.5 – 1 keV flux and a “hard” band ( $H$ ) from 1 – 2 keV we define the hardness ratio as;

$$HR = \frac{H - S}{H + S} \quad (1)$$

As explained above, our sample was initially selected by excluding the data below 0.5 keV to allow a higher efficiency in source detection. We therefore ignore the very soft flux in the first instance and define our hardness ratios from 0.5 – 2 keV in order to characterize the source population fairly without a preferential selection of hard sources.

To test for possible systematic biases that might arise due to the combined energy and radial dependence of the PSF the entire sample was split into sources lying within a 10 arcminute radius from the centre of the PSPC and those lying beyond. No trend in hardness ratios with off-axis angle was apparent at any flux, as verified by a Kolmogorov Smirnov test on the data. Another potential problem in analysing *mean* hardness ratios would be an artificial skewness in the distribution at faint X-ray flux. If the instrument is more sensitive in either the  $H$  or  $S$  bands, individual hardness ratios may be skewed towards +1 or -1 as the flux tends to zero and becomes dominated by noise. To overcome this, we will plot hardness ratios of the *stacked* spectra in each flux bin. However, the similarity of these distributions to those obtained with mean hardness ratios suggest that this problem does not significantly affect our data.

Removing the known galactic stars, BL Lac candidates and the cluster emission<sup>†</sup>, we plot the stacked hardness ratios for the other 313 X-ray sources on Figure 1, binned as a function of flux. These results show a hardening of the mean source spectra with decreasing flux, as previously suggested by Hasinger et al (1993) and Vikhlinin (1994).

Since AGN are the main contributors to the total source flux at brighter energies (eg. Shanks et al 1991), there have been suggestions that an evolution in AGN X-ray spectra may be responsible for the trend in hardness ratios. A hardening of QSO spectra towards higher redshift has been postulated, due to either a change in the actual intrinsic spectrum (Morisawa et al 1995) or the effect of intervening absorption from damped Ly $\alpha$  systems (Vikhlinin et al 1995). On Figure 2(a) we plot the individual hardness ratios, separating QSOs from the other, mostly unidentified sources. The dominant feature on this diagram is the large spread in hardness ratios towards fainter fluxes due to counting statistics. We therefore bin these hardness ratios according to flux, and Figure 2(b) displays the hardness ratios for the stacked spectra in 4 flux bins.

Several features are immediately apparent from these distributions. They show that the unidentified sources have harder mean X-ray spectra than QSOs, regardless of source intensity. A Kolmogorov-Smirnov test yields a  $> 99.9\%$  probability that the two distributions shown on Figure 2(a) do not arise from the same parent population. This is consistent with the errors on the stacked spectra shown on Figure 2(b). Secondly, the *QSOs show no evidence for spectral hardening with decreasing flux*, indicating that the change in mean source spectra is due to the emergence of another population from within the unidentified sources with a harder spectrum than QSOs. Given the incomplete spectroscopic identification in our survey, the unidentified population almost certainly contains some contribution from steep spectrum QSOs. The mean spectrum of the remaining popula-

<sup>†</sup> Note that replacing these sources has a negligible affect on any of the results presented here.

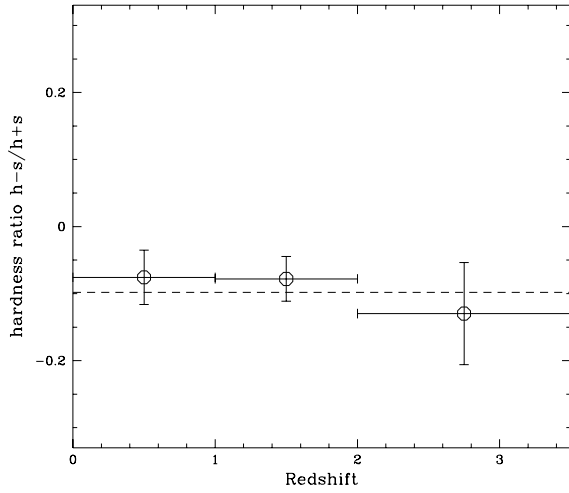
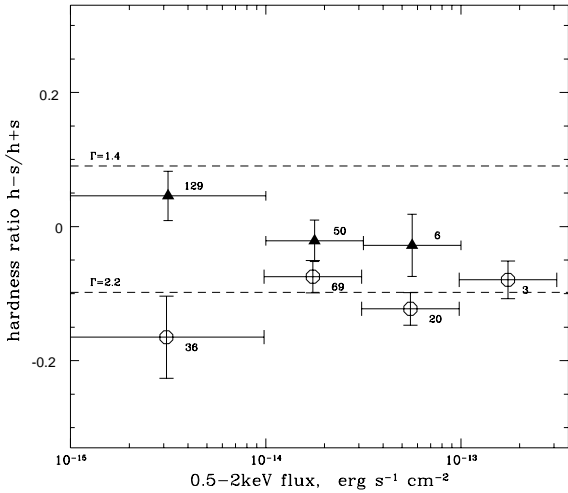
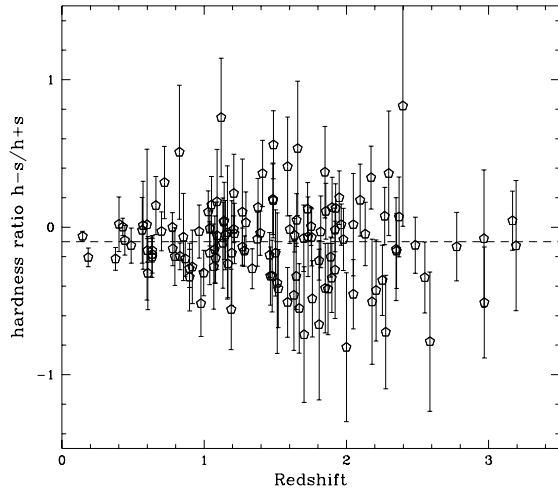
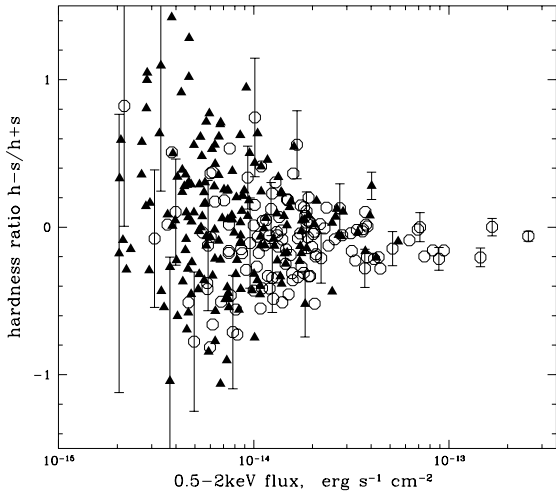


**Figure 2.** (a) Individual 0.5–2 keV hardness ratios as a function of flux for QSOs (unfilled circles) and unidentified X-ray sources and galaxies (filled triangles). For clarity, the appropriate  $1\sigma$  errors are only displayed for a representative selection of sources. On (b) we plot hardness ratios for stacked spectra binned according to flux, as on Figure 1, but separating the QSOs from the unidentified sources and galaxies. Note the change in scale compared to (a).

tion may therefore be even harder than indicated on Figure 2. It is also worth noting that the total spectrum of the unidentified sources harden below  $1 \times 10^{-14} \text{ erg s}^{-1} \text{ cm}^{-2}$ . This may in part be due to a decreasing fractional contamination by unidentified QSOs, but it is interesting to note that this behaviour is predicted by models which explain the residual XRB using a population of sources with curved X-ray spectra (Boyle 1996). The increased contribution from high redshift objects would produce a steep  $\log N$ - $\log S$  relationship for the unidentified population and harden the mean spectra at faint fluxes.

**Figure 3.** (a) Showing hardness ratios as a function of redshift for the 128 QSOs detected on these fields, while (b) shows the stacked hardness ratios when binned according to redshift with  $1\sigma$  errors representing the rms error on the mean. The dotted line shows the mean QSO hardness ratio.

On Figures 3(a) and 3(b) we also plot QSO hardness ratios as function of redshift. This also illustrates the lack of spectral evolution in our QSO sample from 0.5–2 keV, suggesting that broad-line AGN are unlikely to account for the missing hard component of the cosmic XRB. Interestingly however, in the softer band below 0.5 keV (where the cosmic X-ray background is dominated by galactic emission) there does appear to be evidence for a change in QSO spectra with redshift. In this band it is now widely accepted (see Mushotzky et al 1993) that the spectra of QSOs have a significant contribution from a soft excess component, generally believed to be thermal emission from an accretion disk. Using the same sample of QSOs in an independent analy-

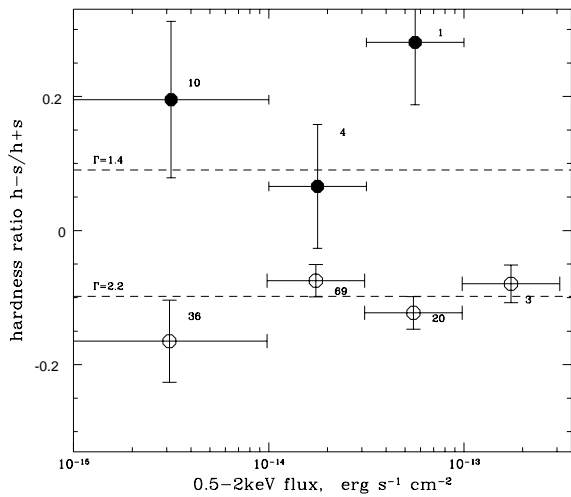
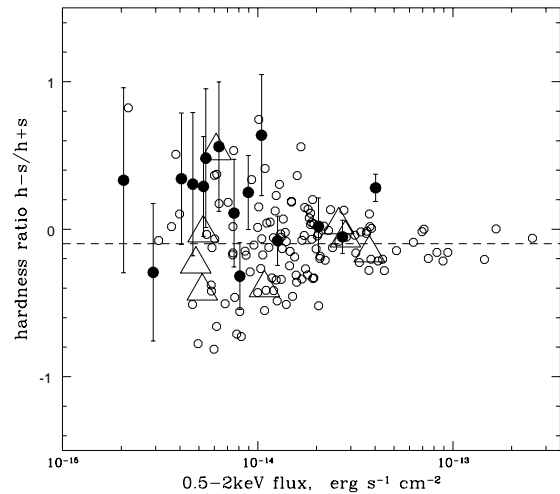


**Figure 4.** (a) Hardness ratios as a function of flux for the 23 most likely X-ray emitting galaxies with the sample of 128 QSOs (unfilled circles) for comparison. Galaxies are separate into 8 absorption line objects (unfilled triangles) and 15 narrow emission line galaxies (filled circles). For clarity the  $1\sigma$  error bars are only displayed for the emission-line galaxies. On (b) we show the hardness ratios for the stacked spectra of the emission line galaxies and QSOs as a function of flux.

sis, Stewart et al (1994) find evidence for a hardening in the spectra of QSOs with redshift in this softer band which has been attributed to changes in the thermal black-body component (see also Mushotzky et al 1993). This evolution is due in part to a redshifting of the soft excess component out of the *ROSAT* passband for higher redshift QSOs, but there also appears to be evidence for a change in the temperature and normalisation of this component. However, we are concerned here with the extragalactic X-ray background above 0.5keV and in this band there is no evidence for any QSO spectral evolution.

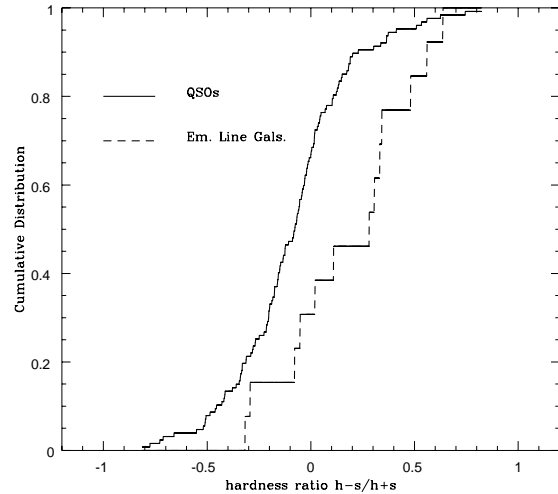


**Figure 5.** Cumulative probability distributions for the 15 emission line galaxies and 128 QSOs shown on Figure 4(a) (Kolmogorov-Smirnov test).

### 3.2 X-ray luminous galaxies

In Section 2 we noted that  $\sim 100$  of the 185 unidentified sources appear to be associated with faint optical galaxies. The cross-correlation results of Roche et al 1995a suggest that many of these are likely to be genuine X-ray sources but due to the high sky density of “normal” field galaxies at faint magnitudes there will also be a significant number of chance associations. We therefore selected a restricted sample of the most likely galaxy candidates with brighter optical magnitudes ( $B < 21.5$ ) and lying within  $20''$  of the X-ray source. In total, 23 galaxies meet this criteria from which we expect only  $\sim 6$  to be spurious identifications (see Section 2.1). The hardness ratios for these X-ray sources and the 128 QSOs are displayed on Figure 4(a), separating the 15 narrow emission line galaxies from the 8 absorption line galaxies. Despite the limited sample and the large errors on individual faint sources, there is clearly evidence that the emission line galaxies in particular come from a harder population than the QSOs. While the 8 absorption line galaxies are evenly distributed about the mean hardness ratio for QSOs, 13 of the 15 emission line galaxies lie formally above this mean value. On Figure 4 (b) we display the hardness ratios for QSOs and emission line galaxies binned according to flux. A Kolmogorov-Smirnov test yields a 98.6% probability that the hardness ratios associated with the emission line galaxies and QSOs do not arise from the same parent population. The cumulative distributions are shown on Figure 5.

**Table 2.** Summary of *ROSAT* fields, with coordinates in J2000 and galactic column density in  $10^{20}$  atom cm $^{-2}$ .

Field	RA	DEC	$N_H$	Exposure time
GSGP4	00 57 28.7	-27 38 24	1.8	48955
SGP2	00 52 04.8	-29 05 24	1.8	24494
SGP3	00 55 00.0	-28 19 48	1.8	21062
QSF1	03 42 09.6	-44 54 36	1.7	26144
QSF3	03 42 14.3	-44 07 48	1.7	27358

## 4 SPECTRAL FITTING

### 4.1 Stacked spectra

In Section 3 we used hardness ratios to analyse the X-ray spectra of individual faint sources. In this section we analyse the X-ray spectra in more detail using the full resolution of the PSPC detector by stacking together the spectra of different source types.

Details of the five *ROSAT* fields used in this analysis are summarised in Table 2. The column densities of galactic hydrogen are very similar on each field, but a mean value weighted by exposure times was used if any stacked spectra were obtained from different fields. For the spectral fitting, the response matrix DRM\_06 was used for observations made before October 1991 (QSF1 and QSF3) while the matrix DRM\_036 was used for observations made after that date (SGP2, SGP3 and GSGP4). Although problems in the calibration of the PSPC (see Turner et al 1995) can lead to some uncertainties in the spectral fits, we are primarily concerned with broad *differences* between the spectra of different sources which should be unaffected by these problems.

Using the XSPEC spectral analysis package, we attempt fitting power-law models (modified only by galactic absorption) to the stacked spectra of QSOs, unidentified X-ray sources and the subset of probable galaxies. We emphasize that no particular physical significance should be attributed to these models and we are merely attempting to parameterise the spectral differences between the source types. For comparison with the hardness ratio analysis in section 3 we also perform the fits using only the 0.5–2keV data. The results (see Table 3) confirm that the unidentified sources, on average, have a harder spectrum than QSOs. In agreement with the hardness ratio analysis, the subset of probable X-ray emitting galaxies (emission line galaxies in particular) appear to have a significantly harder spectrum than QSOs. The raw channel spectra for the QSOs, unidentified sources and the subset of narrow-line X-ray galaxies are displayed on Figure 6 with the best fitting power-law models.

Treating each of the 5 *ROSAT* fields separately, Table 4 displays the results of power-law fits to the stacked spectra of QSOs and unidentified sources. On 4 of the 5 fields there are significant spectral differences between the spectra. Note that the largest difference comes from the deepest (49ks) exposure on the GSGP4 field while on the shortest (21ks) exposure on SGP3 the difference in spectra is negligible, consistent with the picture that a harder population is emerging at fainter fluxes.

As Tables 3 and 4 show, a simple power-law is a reasonable fit to all the stacked data above 0.5keV for all source types. For the full band 0.1–2keV fits however, the values

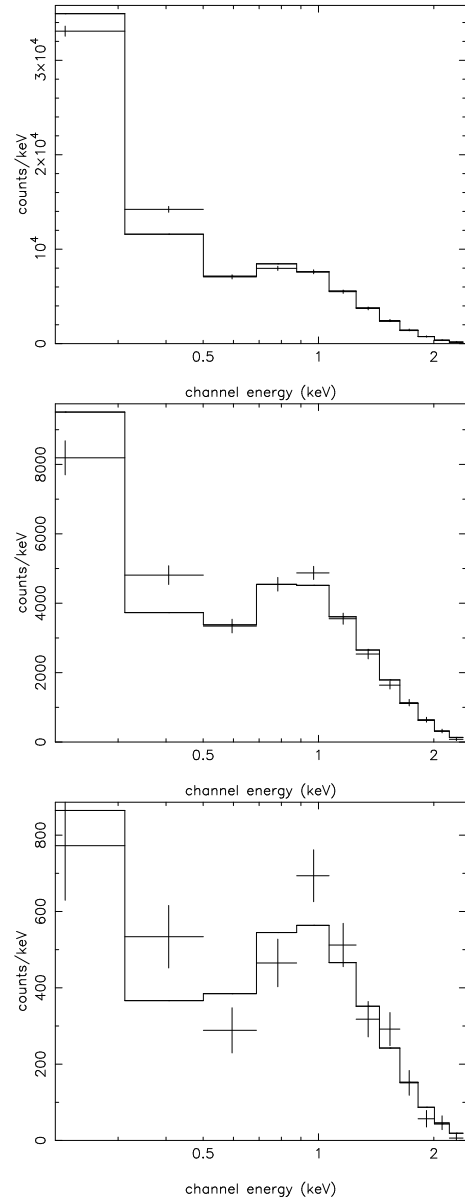


**Figure 6.** The stacked 0.1–2.0 keV X-ray spectra with the best fitting power-law models for (a) the 128 QSOs ( $\Gamma = 2.30 \pm 0.01$ ), (b) the 185 unidentified X-ray sources ( $\Gamma = 1.74 \pm 0.03$ ) and (c) the 15 probable narrow emission-line galaxies identified as a subset of (b) ( $\Gamma = 1.51 \pm 0.09$ ). In each case the photoelectric absorption was fixed at the mean galactic value.

of  $\chi^2_{\text{red}}$  suggest that more detailed models are required to fit the data. For the QSOs in particular, a soft excess component is required below 0.5keV, as described by Stewart et al (1994), but since we are interested only in their contribution to the extragalactic XRB we make no attempt to model this here. Since the 0.5–2.0 keV hardness ratios for QSOs remain constant with redshift this would indicate that we are dealing with a power-law spectrum above 0.5 keV without a significant contribution from a soft excess component.

**Table 3.** Results of power-law fits to the stacked spectra from all fields, separated according to QSOs, unidentified sources and the subset of probable galaxies. Fits are performed with the full 0.1 – 2.0 keV *ROSAT* band and the restricted 0.5 – 2.0 keV for comparison with hardness ratios. Values of photoelectric absorption are fixed at the mean galactic value.

Energy	Source Type	No.	$\Gamma$	$\chi^2_{\text{red}}$
0.5 – 2.0 keV	QSOs	128	2.23±0.04	0.51
	Unidentified	185	1.81±0.06	0.95
	Probable galaxies	23	1.64±0.14	1.18
	(Em. line gal.)	15	1.36±0.18	1.91
	(Abs. line gal.)	8	2.21±0.23	1.25
0.1 – 2.0 keV	QSOs	128	2.30±0.01	8.70
	Unidentified	185	1.74±0.03	3.17
	Probable galaxies	23	1.69±0.06	1.45
	(Em. line gal.)	15	1.51±0.09	1.79
	(Abs. line gal.)	8	1.94±0.08	1.02

**Table 4.** Results of power-law fits to the stacked spectra from each field, fixing the photoelectric absorption to the galactic values shown in Table 2. The fits are also performed using only the 0.5 – 2.0 keV data.

Energy	Field	QSOs		Unidentified	
		$\Gamma$	$\chi^2_{\text{red}}$	$\Gamma$	$\chi^2_{\text{red}}$
0.5 – 2.0 keV	GSGP4	2.13±0.08	1.52	1.65±0.11	1.08
	SGP2	2.16±0.11	1.56	1.74±0.15	1.01
	SGP3	2.38±0.10	1.43	2.30±0.13	0.89
	QSF1	2.19±0.12	1.44	1.84±0.19	0.25
	QSF3	2.44±0.11	1.98	1.71±0.17	1.69
0.1 – 2.0 keV	GSGP4	2.08±0.03	5.63	1.36±0.07	3.83
	SGP2	2.28±0.03	4.65	1.63±0.07	2.37
	SGP3	2.27±0.03	3.84	2.23±0.04	0.96
	QSF1	2.41±0.03	2.11	1.85±0.09	0.30
	QSF3	2.64±0.03	1.98	1.95±0.07	1.68

## 4.2 Individual galaxy spectra

The stacked spectra for the X-ray luminous galaxies appear to be significantly flatter than the combined spectra for the QSOs in our survey. While most of the individual sources yield a total of fewer than 40 X-ray photons in the 0.1 – 2.0 keV band, it is important to establish whether the combined spectrum is due to individual spectra that are intrinsically flat (Di Matteo & Fabian 1996) or alternatively a superposition of absorbed X-ray spectra with correspondingly distinct low energy cutoffs (Comastri et al 1995, see also Almaini et al 1995).

In Table 5 we show the results of individual power-law fits (with galactic absorption) to the X-ray spectra of the 9 brightest X-ray emitting galaxies with a 0.5 – 2.0 keV flux  $> 1 \times 10^{-14} \text{ erg s}^{-1} \text{ cm}^{-2}$ . Spectral fitting becomes increasingly meaningless for the fainter objects which were therefore stacked before spectra fitting. Alternatively, equivalent photon indices from the hardness ratios on Figure 4 are given for these fainter galaxies.

A power law model gives a reasonable fit to 7 of the 9 brightest galaxies and to the stacked spectra of the fainter galaxies. For 2 galaxies however (GSGP4X:091 and GSGP4X:069), simple power-law models do not give an ac-

ceptable fit to the data. Both of these are emission line galaxies and they both show very hard X-ray spectra with  $\Gamma < 1$ .

- **GSGP4X:091** For this object, the brightest of the galaxy candidates, a power-law plus galactic absorption model gives a very flat  $\Gamma=0.145$  but is not a good fit to the data ( $\chi^2_{\text{red}}=2.73$ ). A thermal Raymond-Smith model also gives a very poor fit to the data. The lack of photons at soft energies seems to indicate photoelectric absorption. We therefore try adding an absorbing column at the redshift of the galaxy ( $z = 0.416$ ) and assume an intrinsic power-law of  $\Gamma=2.2$  (the mean value for QSOs). This gave a much improved fit with an intrinsic column density of  $N_H = 7.5 \pm 1.8 \times 10^{21} \text{ atom cm}^{-2}$  ( $\chi^2_{\text{red}}=0.97$ ). The channel spectrum and best fitting model are shown on Figure 7(a).<sup>†</sup> The X-ray spectrum therefore presents strong evidence that this is a highly luminous, obscured X-ray source with an unobscured 0.5 – 2 keV rest-frame luminosity of  $\sim 1.3 \times 10^{44} \text{ erg s}^{-1}$  ( $H_0 = 50 \text{ km s}^{-1} \text{ Mpc}^{-1}$ ,  $q_0 = 0.5$ ).

- **GSGP4X:069** A power-law with only galactic absorption gives a very flat  $\Gamma=0.79$ , but this is not a good fit to

<sup>†</sup> Note that an equally good fit can be obtained with a similar degree of obscuration and a thermal Raymond-Smith model with a temperature of  $\sim 2 \text{ keV}$ .

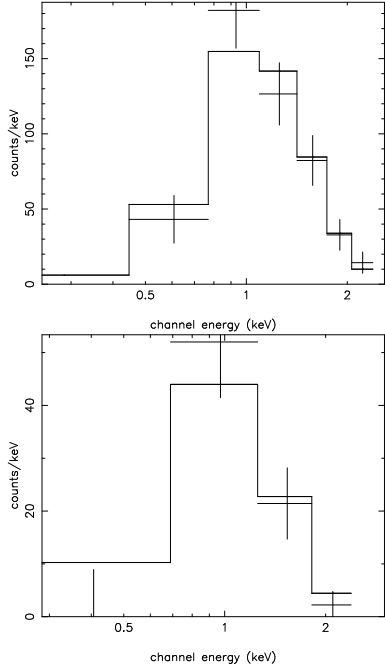


**Figure 7.** 0.1 – 2.4 keV X-ray spectra for the absorbed narrow-emission line galaxies GSGP4X:091 (a) and GSGP4X:069 (b). The models shown are obtained by fixing the intrinsic power law at  $\Gamma = 2.2$  and allowing the restframe absorption to vary.

the data ( $\chi^2_{\text{red}} = 3.62$ ). This faint source has only 46 photons from 0.5 – 2.0 keV but nevertheless it also shows evidence for photoelectric absorption at low energies. Repeating the background subtraction with various source free regions near the source confirms that this is not a systematic effect. Adding an absorbing column at the redshift of the galaxy ( $z = 0.213$ ) and fixing the intrinsic power-law component to  $\Gamma = 2.2$  gave a much improved fit to the data ( $\chi^2_{\text{red}} = 0.53$ ) with a restframe absorbing column of  $N_H = 2.7 \pm 1.9 \times 10^{21} \text{ atom cm}^{-2}$ . The channel spectrum and best fitting absorbed model are shown on Figure 7(b).

While only these 2 galaxies *require* additional absorption above the galactic value, many of the remaining galaxies fit power-law X-ray spectra significantly flatter than QSOs. It would be interesting to determine if these galaxies are intrinsically flat or whether this is also due to obscuration. Unfortunately there are insufficient photons to provide useful constraints on both the power-law index and the rest-frame absorption. Co-adding the fainter spectra does not resolve this ambiguity. Stacking the 14 faintest galaxies with flux  $S_{(0.5-2\text{keV})} < 1 \times 10^{-14} \text{ erg s}^{-1} \text{ cm}^{-2}$ , we obtain a good fit with an unabsorbed power law of index  $\Gamma = 1.68 \pm 0.11$  ( $\chi^2_{\text{red}} = 0.83$ ). An equally good fit is obtained with an intrinsic QSO-like power law ( $\Gamma = 2.2$ ) and a low level of additional photoelectric absorption ( $N_H \sim 1 \times 10^{21} \text{ atom cm}^{-2}$ ). We conclude that further data are required to differentiate between these possibilities.

## 5 SUMMARY AND CONCLUSIONS

Using a sample of over 300 X-ray sources detected on 5 deep (21-49ks) *ROSAT* fields we investigate the X-ray spectra

of the source population. Using a hardness ratio analysis we confirm recent claims that the average source spectra harden towards fainter fluxes from an equivalent photon index of  $\Gamma = 2.2$  at  $S_{(0.5-2\text{keV})} = 1 \times 10^{-13} \text{ erg s}^{-1} \text{ cm}^{-2}$  to  $\Gamma \simeq 1.7$  below  $1 \times 10^{-14} \text{ erg s}^{-1} \text{ cm}^{-2}$ . We then attempt to show the type of source responsible for this trend. So far 128 QSOs have been identified from this survey and these dominate the source counts at X-ray fluxes above  $1 \times 10^{-14} \text{ erg s}^{-1} \text{ cm}^{-2}$ . At fainter fluxes the X-ray population remains largely unidentified. We find that the unidentified sources have harder mean X-ray spectra than QSOs, regardless of source intensity. We also show that the QSOs detected so far show no evidence for spectral hardening with decreasing flux, implying that the change in mean spectra is due to the emergence of another source population. Recent work has suggested that many of these are X-ray luminous galaxies (Roche et al 1995a, Boyle et al 1995a, Carballo et al 1995, McHardy et al 1995). Taking a subset of 23 X-ray sources identified as the most likely galaxy candidates, we find that these show a mean spectral index of  $\Gamma = 1.69$  from 0.1 – 2.0 keV, confirming the findings of Carballo et al 1995. These galaxies consist of 8 absorption-line galaxies and 15 with emission line features. Hardness ratios suggest that the emission-line galaxies have significantly harder X-ray spectra than QSOs. Stacking the spectra of these faint sources, the absorption-line galaxies yield a spectral index of  $\Gamma = 1.94 \pm 0.08$  while the emission-line galaxies give  $\Gamma = 1.51 \pm 0.09$  from 0.1 – 2.0 keV, more consistent with the residual X-ray background. Individually, the galaxies show a range of spectral properties from very hard X-ray sources to those with soft, QSO-like spectra. At least 2 emission-line galaxies show evidence for significant photoelectric absorption in the range  $N_H \sim 10^{21} - 10^{22} \text{ atom cm}^{-2}$ . Given recent results which suggest that the surface density of narrow emission-line galaxies could approach that of AGN at  $\sim 1 \times 10^{-15} \text{ erg s}^{-1} \text{ cm}^{-2}$  and possibly contribute 15 – 40% of the total XRB at 1 keV (Boyle et al 1995a, Griffiths et al 1995b), these spectral results provide further evidence that they may be the missing component of the cosmic XRB.

## ACKNOWLEDGMENTS

OA was funded by an SERC/PPARC studentship. BJB was partly supported by a Royal Society University Research Fellowship during part of this work. OA thanks Andy Fabian for helpful advice and discussions. We also thank the staff at the Anglo-Australian observatory and the *ROSAT* team for making these observations possible.

## REFERENCES

- Almaini O., Boyle B.J., Griffiths R.E., Shanks T., Stewart G.C. & Georgantopoulos I., 1995, MNRAS 277, L31
- Almaini O. 1996, Ph.D. thesis
- Boyle B.J., Jones L.R., & Shanks, T., 1991 MNRAS 251, 482
- Boyle B.J., McMahon R.G., Wilkes B.J., & Elvis M., 1995a, MNRAS 272, 462
- Boyle B.J., McMahon R.G., Wilkes B.J., & Elvis M., 1995b, MNRAS 276, 315
- Boyle B.J., 1996, Observatory 116, 11
- Carballo R. et al 1995, MNRAS 277, 1312

**Table 5.** Summary of the 23 probable X-ray emitting galaxies with  $0.1 - 2.0$  keV spectral fits for the 9 brightest sources and the stacked spectra of the fainter galaxies. The equivalent photon index from a hardness ratio is also quoted for the faintest galaxies. Optical and X-ray coordinates are given in B1950 format. A power-law fit is performed with the photoelectric absorption fixed at the galactic value. The  $0.5 - 2$  keV flux is given in  $\text{erg s}^{-1} \text{cm}^{-2}$ . Column 7 gives the offset between the X-ray source and optical galaxy in arcseconds. Column 10 gives the  $b_j$  magnitude of the galaxy. Note that  $\sim 6$  of these galaxies will be chance associations with X-ray sources.

Source	RA <sub>x</sub>	Dec <sub>x</sub>	Flux	$\Gamma$	$\chi^2_{\text{red}}$	$d_{ox}$	RA <sub>o</sub>	Dec <sub>o</sub>	$b_j$	Em/Abs
GSGP4X : 091	00 55 36.8	-28 09 15	$4.0 \times 10^{-14}$	$0.14 \pm 0.30$	2.77	10.4	00 55 36.3	-28 09 23	21.33	Em
GSGP4X : 017	00 54 08.7	-27 46 23	$3.7 \times 10^{-14}$	$2.25 \pm 0.09$	1.24	17.2	00 54 08.5	-27 46 06	18.27	Abs
QSF1X : 020	03 39 41.5	-45 21 07	$2.8 \times 10^{-14}$	$1.95 \pm 0.21$	0.33	14.5	03 39 42.4	-45 21 18	19.66	Abs
GSGP4X : 048	00 54 51.6	-27 37 49	$2.7 \times 10^{-14}$	$1.82 \pm 0.15$	1.83	11.3	00 54 51.8	-27 38 00	20.37	Em
SGP3X : 006	00 51 38.6	-28 40 46	$2.5 \times 10^{-14}$	$1.62 \pm 0.18$	0.64	15.0	00 51 38.2	-28 40 32	18.78	Abs
QSF1X : 036	03 40 08.3	-44 48 14	$2.0 \times 10^{-14}$	$2.49 \pm 0.18$	0.67	10.9	03 40 07.9	-44 48 24	21.07	Em
GSGP4X : 069	00 55 12.2	-27 49 19	$1.3 \times 10^{-14}$	$0.79 \pm 0.51$	3.67	9.4	00 55 11.5	-27 49 17	20.25	Em
GSGP4X : 064	00 55 07.1	-27 39 30	$1.2 \times 10^{-14}$	$1.73 \pm 0.35$	0.65	9.5	00 55 06.4	-27 39 32	17.84	Abs
SGP3X : 033	00 52 36.3	-28 54 37	$1.0 \times 10^{-14}$	$1.94 \pm 0.24$	0.63	17.0	00 52 35.2	-28 54 46	18.86	Em
Faint(14)	-	-	$< 1.0 \times 10^{-14}$	$1.68 \pm 0.11$	0.83	-	-	-	-	-
GSGP4X : 114	00 56 11.5	-28 04 41	$8.6 \times 10^{-15}$	$1.22 \pm 0.51$ *	-	19.0	00 56 11.4	-28 05 00	18.93	Em
GSGP4X : 094	00 55 42.0	-27 50 40	$7.7 \times 10^{-15}$	$2.55 \pm 0.48$ *	-	8.1	00 55 41.9	-27 50 48	20.22	Em
SGP2X : 060	00 50 25.2	-29 13 38	$7.4 \times 10^{-15}$	$1.44 \pm 0.65$ *	-	9.0	00 50 25.2	-29 13 29	21.27	Em
SGP2X : 025	00 49 25.9	-29 20 45	$6.3 \times 10^{-15}$	$-0.2 \pm 0.82$ *	-	9.1	00 49 25.8	-29 20 36	21.06	Em
SGP2X : 049	00 49 51.9	-29 25 43	$6.1 \times 10^{-15}$	$0.02 \pm 0.90$ *	-	17.8	00 49 52.5	-29 25 59	20.67	Abs
QSF1X : 064	03 41 26.7	-45 04 44	$5.4 \times 10^{-15}$	$0.15 \pm 1.10$ *	-	16.1	03 41 27.6	-45 04 31	20.20	Em
GSGP4X : 109	00 55 59.7	-27 45 27	$5.3 \times 10^{-15}$	$0.77 \pm 1.15$ *	-	8.8	00 55 59.3	-27 45 34	16.78	Em
GSGP4X : 086	00 55 31.1	-27 40 45	$5.3 \times 10^{-15}$	$1.72 \pm 0.82$ *	-	7.1	00 55 31.2	-27 40 38	17.94	Abs
QSF3X : 039	03 40 30.1	-44 27 15	$5.2 \times 10^{-15}$	$2.57 \pm 0.95$ *	-	6.4	03 40 29.5	-44 27 15	19.57	Abs
GSGP4X : 020	00 54 16.0	-28 03 12	$4.8 \times 10^{-15}$	$2.95 \pm 1.12$ *	-	7.9	00 54 16.6	-28 03 12	21.43	Abs
QSF1X : 033	03 40 08.5	-45 10 17	$4.7 \times 10^{-15}$	$0.65 \pm 1.62$ *	-	19.3	03 40 10.3	-45 10 20	19.57	Em
GSGP4X : 082	00 55 24.6	-27 39 27	$4.1 \times 10^{-15}$	$0.59 \pm 1.54$ *	-	9.1	00 55 24.5	-27 39 18	18.88	Em
GSGP4X : 054	00 54 55.5	-28 01 06	$2.9 \times 10^{-15}$	$2.69 \pm 1.61$ *	-	8.0	00 54 55.9	-28 01 00	19.96	Em
GSGP4X : 057	00 54 59.3	-27 59 48	$2.1 \times 10^{-15}$	$0.62 \pm 2.30$ *	-	20.0	00 55 00.8	-27 59 50	19.52	Em

\* Equivalent photon index from the  $0.5 - 2.0$  keV hardness ratio

Comastri A., Setti G., Zamorani G. & Hasinger G., 1995, A&A, 296, 1

Di Matteo T. & Fabian A.C. 1996, MNRAS Submitted

Gendreau K.C. et al, 1995, Publ. Astron. Soc. Japan, 47, L5-L9

Georgantopoulos I., Stewart G.C., Shanks T., Griffiths R.E., & Boyle B.J., 1993, MNRAS 262, 619

Georgantopoulos I., Stewart G.C., Shanks T., Griffiths R.E., & Boyle B.J., 1996, MNRAS 280, 276

Griffiths R.E., Georgantopoulos I., Boyle B.J., Stewart G.C., Shanks T., Della Ceca R., 1995a, MNRAS 275, 77

Griffiths R.E., Della Ceca R., Georgantopoulos I., Boyle B.J., Stewart G.C., Shanks T. & Fruscione A., 1995b, MNRAS 281, 71

Hasinger G., Turner J.T., George I.M., Boese G., 1992, GSFC Calibration Memo CAL/ROS/92-001

Hasinger G., Burg R., Giacconi R., Hartner G., Schmidt M., Trümper J., Zamorani G., 1993, A&A, 275, 1

McHardy I. et al., 1995, Spectrum 6, 11

Metcalfe N., Shanks T., Fong R., Jones L.R., 1991, MNRAS 249, 498

Morisawa K. et al A&A 236, 299

Mushotzky R.F., Done C., Pounds K.A., 1993, Ann. Rev. Astr. Ap., 31, 717

Roche N., Shanks T., Georgantopoulos I., Stewart G.C., Boyle B.J., & Griffiths R.E., 1995a, MNRAS 273, L15

Roche N., Shanks T., Almaini O., Boyle B.J., Georgantopoulos I., Stewart G.C., & Griffiths R.E., 1995b, MNRAS 276, 706

Plucinsky P.P., Snowden S.L., Briel U.G., Hasinger G., Pfeffermann E., 1993, ApJ 418, 519

Shanks T., Georgantopoulos I., Stewart G.C., Pounds K.A., Boyle B.J. & Griffiths R.E., 1991 Nat 353, 315

Snowden S.L., Freyberg M.J., 1993, ApJ 404, 403

Stewart G.C., Georgantopoulos I., Boyle B.J., Shanks T., Griffiths R., 1994, New Horizon Of X-ray Astronomy - first results from ASCA, p331, eds. F. Makino and T. Ohashi, Universal Academy Press, Tokyo

Turner T.J., 1993, GSFC Calibration Memo CAL/ROS/93-007

Vikhlinin A., Forman W., Jones C. & Murray S., 1995 ApJ 451, 564